NICOLAUS COPERNICUS UNIVERSITY IN TORUŃ

Bulletin of Geography. Physical Geography Series, No. 30 (2026): 25–37
http://doi.org/10.12775/bgeo-2026-0002

Drought risk assessment in Quang Tri Province, Vietnam using Landsat multi-temporal remote sensing data and machine learning algorithm

Thi Thu Trang Tran[1] [a], Le Hung Trinh[2] *[b], Thi Phuong Thao Do[3] [c], Van Phu Le[4]

[1,3]Hanoi University of Mining and Geology, Hanoi, Vietnam
[2,4]Le Quy Don Technical University, 236 Hoang Quoc Viet Street, Hanoi, Vietnam

*Correspondence e-mail: trinhlehung@lqdtu.edu.vn

[a]https://orcid.org/0009-0007-1135-0865, [b]https://orcid.org/0000-0002-2403-063X, [c]https://orcid.org/0009-0008-9464-8831

Abstract. Drought is a major environmental challenge that significantly impacts agriculture, water resources and ecosystems, particularly in regions prone to arid conditions. This study aims to classify and monitor drought severity using multi-temporal remote sensing data, drought indices and machine learning techniques. Landsat satellite imageries from 2014 to 2024, collected at two-year intervals, are utilized to assess drought patterns in Quang Tri Province, Vietnam. Three key drought indices Normalized Difference Vegetation Index (NDVI), Normalized Difference Water Index (NDWI) and Land Surface Water Index (LSWI) are computed to evaluate vegetation health, surface water content and soil moisture levels. The Random Forest algorithm on Google Earth Engine (GEE) is applied to classify drought into different severity levels based on spectral features extracted from satellite images. The results indicate a clear spatial and temporal variation in drought severity, with coastal areas consistently undergoing extreme drought, whereas central regions show increasing drought expansion over time. Western and southern areas remain relatively stable due to higher vegetation cover and water retention capacity. The study highlights the effectiveness of combining remote sensing data and machine learning in improving drought classification accuracy. The findings contribute to early-warning systems, water resource management and climate adaptation strategies, providing valuable insights for policymakers and land managers.

Key words:
Remote sensing,
Landsat,
drought index,
Random Forest,
Quang Tri Province, Vietnam

Introduction

Drought is a severe natural disaster that significantly impacts water resources, agriculture and ecosystems worldwide (Maybank et al. 1995; Sivakumar 2005; Trinh and Vu 2019). Unlike other natural disasters such as floods or hurricanes, drought develops slowly and is difficult to detect in its early stages (Cooley 2006). Its effects are often long-lasting, causing serious damage to food production, water supply and economic stability (Wilhite 2016). With the increasing frequency and severity of droughts due to climate change, accurate monitoring and classification of drought conditions have become crucial for water resource management, agricultural planning and disaster mitigation strategies (Gupta et al. 2011; Wilhite et al. 2014; Kumar et al. 2024).

Remote sensing data have been widely utilized for drought detection and classification due to their ability to provide continuous and objective observations across extensive regions (AghaKouchak et al. 2015; West et al. 2019). Multi-temporal satellite imagery, such as from Landsat and Sentinel-2, enables

researchers to track changes in vegetation health, soil moisture and surface water availability over time (Bhaga et al. 2023). Various spectral indices have proven effective in assessing drought severity by detecting variations in vegetation vigor and water stress. These indices provide critical insights into drought-affected areas, allowing for a more detailed spatial and temporal understanding of drought dynamics (Ihuoma and Madramootoo 2019; Trinh and Vu 2019; Pham et al. 2022; Agarwal et al. 2025). However, despite their effectiveness, these indices alone may not always provide sufficient accuracy in drought classification, particularly when dealing with complex environmental conditions.

To enhance the precision of drought classification, machine learning algorithms have been integrated with remote sensing data and drought indices (Zha et al. 2025). Supervised classification techniques, such as Random Forest (RF) or Artificial Neural Network, have demonstrated high performance in distinguishing different drought severity levels based on a combination of spectral features (Alemu et al. 2025). These algorithms can process large datasets, learn complex patterns in remote sensing imagery and improve classification accuracy by minimizing human bias. By training on labeled sample data, machine learning algorithms can classify drought levels with high precision, making it an ideal choice for large-scale drought monitoring applications (Xiao et al. 2024).

In recent years, Google Earth Engine (GEE) platform has emerged as a powerful cloud-based tool for processing and analyzing large-scale geospatial datasets (Vijayakumar et al. 2024). GEE provides access to a vast repository of satellite imagery and enables real-time data processing using JavaScript or Python APIs (Ghosh et al. 2022). Its capacity to handle multi-temporal and high-resolution imagery makes it highly suitable for drought monitoring and classification tasks. Moreover, GEE allows for the integration of spectral indices and machine learning algorithms directly within the platform, streamlining the workflow from data acquisition to model deployment (Yang et al. 2022). This significantly reduces computational burden and processing time while enabling reproducible and scalable analyses from regional to global levels (Tamiminia et al. 2020; Vijayakumar et al. 2024).

This study aims to develop an integrated drought classification approach that combines multi-temporal remote sensing data, drought indices and machine learning techniques to enhance the accuracy of drought monitoring. The study focuses on classifying drought severity levels using Landsat imagery, spectral indices (NDVI, NDWI, LSWI) and the Random Forest algorithm. All data processing, index calculation and model implementation were conducted on GEE platform, which enabled efficient handling of large datasets and facilitated a streamlined, cloud-based workflow for regional-scale drought assessment.

Materials and methodologys

Study area

Quang Tri is a province in the North Central Coast region of Vietnam, characterized by diverse topography and harsh climatic conditions. Covering an area of approximately 4,739 km², it borders Quang Binh to the north, Thua Thien Hue to the south, Laos to the west, and the East Sea to the east (Electronic Information Portal Of Quang Tri Province 2025). The province's terrain is distinctly divided into three main regions: the mountainous region in the west, the midland hilly area in the center, and the coastal lowlands in the east. The western mountainous region occupies the largest area, featuring high elevations and steep slopes, predominantly along the border with Laos. The midland and hilly areas have infertile soils with low water retention capacity, while the narrow coastal plains are vulnerable to saline intrusion and erosion.

Quang Tri falls within the tropical monsoon climate zone, undergoing two distinct rainy and dry seasons. The rainy season lasts from September to December, with high rainfall averaging between 2,200 and 2,700 mm per year, often leading to flooding and soil erosion. Conversely, the dry season extends from January to August, with the peak dry period occurring between April and August, when the province is heavily affected by the hot, dry Lao winds. These winds not only raise temperatures to extreme levels, sometimes reaching 39–41 °C, but also drastically reduce humidity, accelerating water evaporation and intensifying drought conditions. Additionally, while Quang Tri has major rivers such as the Thach Han and Hieu Rivers, their flow is highly dependent on seasonal rainfall. During the

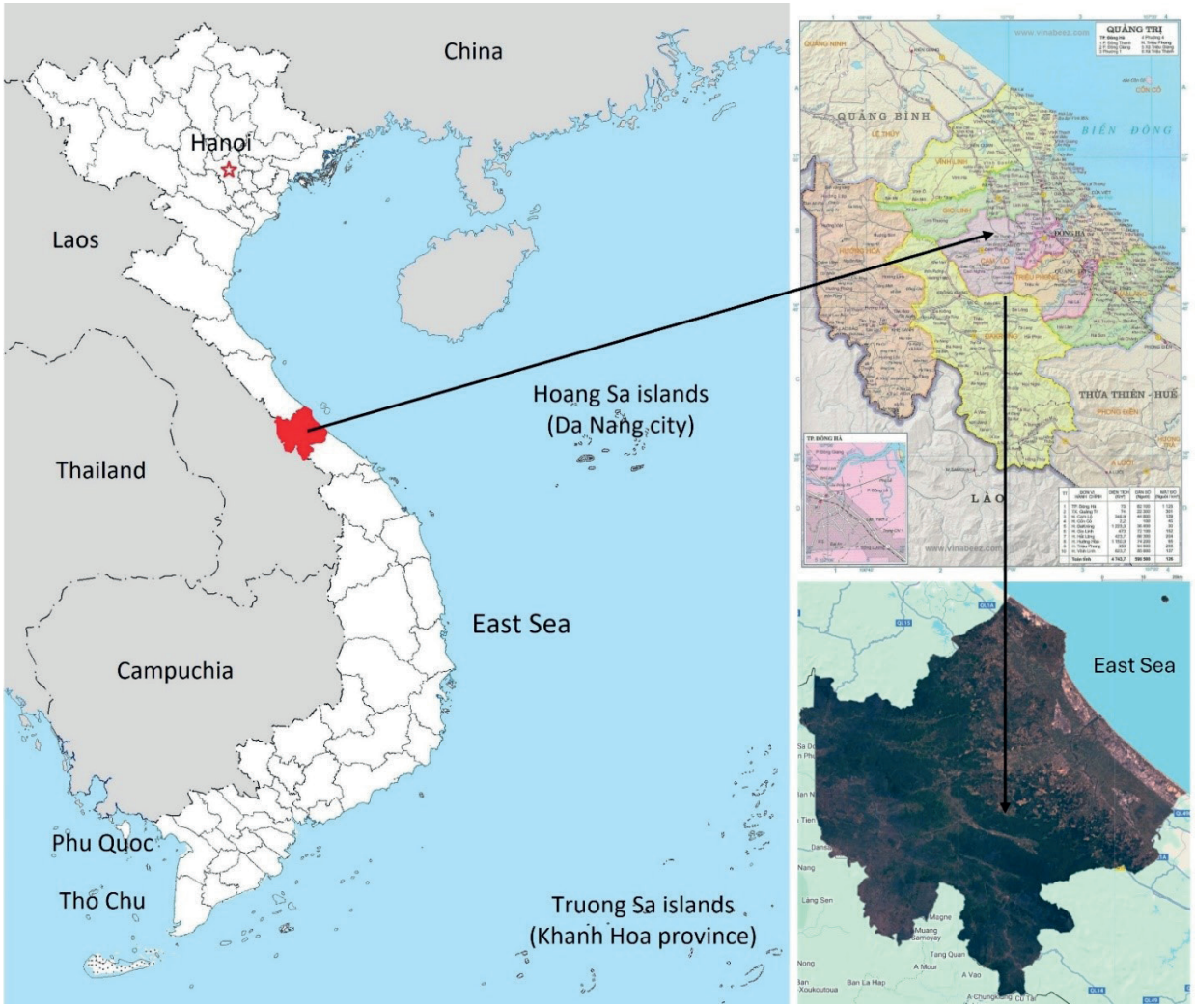

Fig. 1. Location of the study area
Source: Prepared by the authors based on provincial boundary data, the administrative map of Quang Tri province, and Landsat satellite imagery.

dry season, many streams and rivers dry up, exacerbating water shortages for agriculture and daily consumption.

Due to these geographical and climatic characteristics, Quang Tri is one of the most drought-prone provinces in Central Vietnam. Droughts frequently occur during the dry season, significantly impacting agricultural production by reducing crop yields, particularly for rice and industrial crops such as pepper and rubber. The land in the midland and coastal areas is highly susceptible to degradation due to prolonged water shortages, while the coastal zone faces increased risks of saline intrusion caused by a lack of freshwater resources. Additionally, access to drinking water becomes increasingly difficult, especially in rural areas where the water supply infrastructure is inadequate.

Data sources

The study utilizes multi-temporal Landsat data for drought classification. Landsat is one of the most important data sources for drought monitoring research, providing continuous satellite imagery since 1972. Operated by the National Aeronautics and Space Administration (NASA) and the U.S. Geological Survey (USGS), the Landsat program offers multi-spectral data with a 30-meter spatial resolution, enabling the monitoring of vegetation changes, soil moisture and surface water over time (NASA 2025; U.S. Geological Survey 2025). Different Landsat generations, such as Landsat 5 TM, Landsat 7 ETM+, Landsat 8 OLI/TIRS and Landsat 9 OLI-2/TIRS-2, are widely used in drought studies due to their multi-temporal data acquisition capabilities, with a revisit cycle of 16 days.

In this study, 06 Landsat 8 and Landsat 9 OLI_TIRS images were used to calculate drought indices (NDVI, LSWI, NDWI) for creating a drought-risk map of Quang Tri province. Information about the Landsat 8/9 imagery used in this study is presented in Table 1.

Methodology

The drought classification process using multi-temporal Landsat imagery, drought indices and the Random Forest (RF) algorithm involves multiple steps, including data collection, drought indices computation, sample data generation, data incorporation, drought classification and assessment of affected area changes. Figure 2 illustrates the remote-sensing-data processing workflow adopted in this study for drought classification.

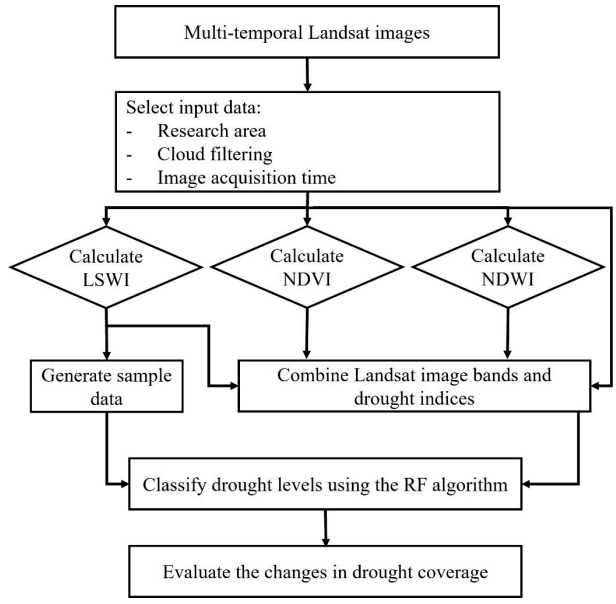

Fig. 2. Flowchart of remote-sensing-data processing in this study

Step 1: Collecting multi-temporal Landsat satellite images

The first step in the process is to collect multi-temporal Landsat satellite images to monitor drought variations over time. This study utilizes Landsat datasets available on the cloud computing platform Google Earth Engine (GEE). The Landsat program has multiple sensor generations, among which Landsat 8 OLI/TIRS and Landsat 9 OLI-2/TIRS-2 are commonly used sources for drought analysis (GEE 2025).

After collecting the dataset, input images are selected and preprocessed. The key factors to determine include the study area, cloud filtering and the image acquisition period.

- Study area: The research defines the boundaries of the study region to focus on processing relevant data.
- Cloud filtering: Since Landsat satellite images can be affected by cloud cover, cloud masking techniques are applied to remove cloud-affected areas and enhance data quality (Guo et al. 2016; Cao et al. 2020).
- Image acquisition period: Drought is a seasonal phenomenon, so images must be collected at different time points to evaluate change trends. This study collects images over the research years, corresponding to the dry season when drought conditions occur in the study area (Table 1).

Table 1. Landsat data used in this study

No.	Satellite	Acquisition date
1	Landsat 8 OLI_TIRS	August 1, 2014
2	Landsat 8 OLI_TIRS	July 21, 2016
3	Landsat 8 OLI_TIRS	May 24, 2018
4	Landsat 8 OLI_TIRS	July 16, 2020
5	Landsat 9 OLI2_TIRS2	August 31, 2022
6	Landsat 9 OLI2_TIRS2	August 4, 2024

Finally, the authors obtain a multi-temporal Landsat image dataset, where each image represents a specific research period.

Step 2: Calculation of the drought indices

After obtaining high-quality input data, the next step is to calculate key indices to assess drought conditions. These indices are essential in determining the extent of water stress, soil moisture availability and overall vegetation health. The primary drought indices used in this study include LSWI, NDVI and NDWI, which are defined as follows:

- LSWI (Land Surface Water Index): LSWI is a key indicator in monitoring drought by assessing soil and vegetation moisture (Dong et al. 2014). It responds quickly to rainfall, making it useful for tracking water availability (Chandrasekar et al. 2010). In low-precipitation areas, LSWI shows a strong correlation with total rainfall. It also helps monitor vegetation health and soil water content across different growth stages, aiding in drought assessment and agricultural planning. LSWI is calculated using the Near-Infrared (NIR) and Shortwave Infrared (SWIR) bands of Landsat imagery as (Mohammed et al. 2024):

$$LSWI = \frac{NIR - SWIR}{NIR + SWIR} \quad (1)$$

- NDVI (Normalized Difference Vegetation Index): NDVI is a widely used indicator in monitoring drought by assessing vegetation health and water stress. NDVI is calculated as (Myneni et al. 1995):

$$NDVI = \frac{NIR - Red}{NIR + Red} \quad (2)$$

- NDWI (Normalized Difference Water Index): First introduced by Gao in 1996, NDWI has become widely used in agriculture, forestry and environmental monitoring to analyze drought effects and water dynamics (Gao 1996). NDWI is particularly valuable for detecting surface water changes, assessing vegetation moisture content and identifying drought-prone areas. The formula for NDWI:

$$NDWI = \frac{Green - NIR}{Green + NIR} \quad (3)$$

In this study, Landsat surface reflectance imagery was processed on the Google Earth Engine (GEE) platform to enable consistent multi-temporal analysis. Landsat 8 and Landsat 9 Collection 2 Level-2 Surface Reflectance datasets, atmospherically corrected using the LaSRC algorithm, were utilized. Cloud and shadow contamination were mitigated through the CFMask band (QA_PIXEL), with an additional buffer applied around flagged pixels to minimize edge effects. To address temporal acquisition differences, a median composite was generated for each dry-season period (May–August), thereby reducing residual atmospheric noise and ensuring seasonal comparability. Spectral indices, including NDVI, LSWI and NDWI, were subsequently derived from the corresponding Landsat bands (Green: B3, Red: B4, NIR: B5, SWIR: B6) to monitor vegetation dynamics and surface moisture. The use of GEE enabled efficient data access, preprocessing and harmonization of multi-year Landsat archives, which is critical for detecting spatiotemporal drought patterns at the provincial scale.

Step 3: Generating sample data and integrating drought indices

After calculating the vegetation indices, the data is aggregated to serve as input for the drought classification model. The LSWI index is specifically used to generate sample data, which is essential for training the model.

LSWI has four levels of severity classification. The first class represents extreme drought, with values in the range of LSWI ≤ –0.1. The second class indicates severe drought, ranging –0.1 < LSWI ≤ 0. The third class corresponds to moderate drought, with values of 0 < LSWI ≤ 0.1. The fourth class represents no drought, with LSWI values in the range of 0.1 < LSWI (Du et al. 2018; Alwan and Aziz 2022).

The sample dataset is generated by randomly selecting 1,000 samples from the extreme drought class of LSWI and labeling them as "drought" and 1,000 samples from the no-drought class of LSWI and labeling them as "no drought". The dataset was subsequently divided into training (70%) and testing (30%) subsets for model performance evaluation. At the same time, all calculated indices from Landsat imagery will be integrated with Landsat spectral bands to form the input dataset, enhancing the accuracy of drought classification. The input dataset

includes NDVI, NDWI, LSWI, BLUE (Band 2), GREEN (Band 3), RED (Band 4), NIR (Band 5), SWIR1 (Band 6) and SWIR2 (Band 7).

Step 4: Drought classification using the RF algorithm

Aggregated data obtained from the previous steps were utilized within the Random Forest (RF) machine learning algorithm to classify drought severity levels. Random Forest (RF) is a robust algorithm capable of effectively handling nonlinear data by integrating multiple decision trees (Breiman 2001). The model was trained on the generated sample dataset and subsequently applied to the entire study area to classify drought into distinct severity levels. This approach enhances the reliability and accuracy of drought classification.

The RF model was trained as a binary classifier with two classes: drought and no-drought. After training, the model outputs the probability of each pixel belonging to the drought class. In Google Earth Engine (GEE), the RF classifier is deployed with 200 trees, the remaining parameters are set to default values. To produce categorical drought severity maps, these probabilities were partitioned into five severity levels using equal intervals:

Extreme drought: $P \geq 0.8$
Severe drought: $0.6 \leq P < 0.8$
Moderate drought: $0.4 \leq P < 0.6$
Mild drought: $0.2 \leq P < 0.4$
No drought: $P < 0.2$

This probability-based discretization allowed the conversion of binary classification outputs into multi-class drought severity levels, ensuring both consistency in training and interpretability in mapping.

Step 5: Assessing drought-affected area changes over time

After classifying drought severity, the final step is to evaluate changes in the drought-affected area over time. Comparing drought data across multiple years helps identify drought trends, determine the most severely affected regions, and assess the spatial extent of drought expansion. This analysis provides crucial insights for understanding drought progression and developing strategies for mitigation and resource management.

Results and discussion

The study collects multi-temporal Landsat images spanning the period from 2014 to 2024, with a two-year interval between each image. The research focuses on Quang Tri Province, enabling a comprehensive assessment of drought patterns and trends over the past decade. Figure 3 presents the collected Landsat images displayed using a natural color composite (Red - Green - Blue).

LSWI maps from 2014 to 2024 show fluctuations in drought severity across Quang Tri Province (Fig. 4). Lower LSWI values in 2020 indicate increased drought stress, whereas 2022 data show slight improvements. Southern and south-western areas consistently exhibit a lower LSWI, suggesting greater drought risk. The variability may be attributed to changes in precipitation, land use, and climatic influences, highlighting the necessity of drought monitoring and the development of adaptive water management strategies. Based on Figure 5, NDVI values in Quang Tri fluctuated significantly during 2014–2024, reflecting changes in land cover and drought conditions. In 2014 and 2016, low NDVI was prevalent in coastal and sand dune areas. In 2018–2020, spatial differentiation was more evident: the plains maintained high NDVI, while hilly and coastal areas remained low. In 2022, the maximum NDVI was 0.86, with the area of low values decreasing, indicating favorable humid conditions. However, in 2024, the minimum NDVI decreased to –0.46, reflecting the return of drought. Similarly, the NDWI values in Quang Tri province during 2014–2024 show clear fluctuations in surface moisture conditions (Fig. 6). In 2014 and 2016, the maximum NDWI reached 0.70 and 0.66, while low values were widespread in coastal areas and dry uplands. In 2018, the index declined sharply, indicating more severe moisture deficiency. By 2020, NDWI slightly recovered but remained lower than the early period. Notably, in 2022, the maximum value reached 0.81, reflecting unusually wet conditions consistent with the peak "no drought" classification. However, in 2024, the maximum dropped to 0.53, indicating reduced moisture and a renewed risk of drought.

Based on the independent test dataset of 600 samples, the RF model for 2024 achieved an overall accuracy (OA) of 0.97 and a Kappa coefficient (κ) of 0.93, indicating a very high level of agreement beyond chance. The confusion matrix shows that 289 drought pixels were correctly classified, 11 drought pixels were misclassified as "no drought", 291 no-drought pixels were correctly classified, and only 9 no-drought pixels were misclassified (Table 2). Class-specific performance metrics were also high, with F1-scores of 0.97 for the drought class and 0.96 for the no-drought class, while both precision and recall ranged from 0.96 to 0.97. These results confirm the balanced and stable classification ability of the RF model and demonstrate the reliability of the approach for drought assessment.

The drought classification maps for Quang Tri Province (2014–2024) reveal significant spatial and temporal variations in drought severity. Over the ten-year period, the eastern coastal region consistently undergoes extreme drought, as indicated by the dominance of red areas. This is likely due to sandy soil with low water retention, high evaporation rates, and saltwater intrusion. The central region, including agricultural and urban areas, shows fluctuating drought intensity, with an expansion of moderate and severe drought conditions over time. This trend may be influenced by land use changes, deforestation and increased water demand for agriculture and human uses. Meanwhile, the western and southern regions remain largely unaffected, as shown by the prevalence of green (no-drought) areas across all years. These areas benefit from higher forest cover, better water retention, and proximity to natural water sources. Over time, drought conditions worsen in 2016 and 2020, reflecting reduced rainfall and increasing climate variability. The maps suggest that coastal areas are the most vulnerable, while central regions are at growing risk of severe drought expansion. Key factors contributing to these trends include climate change, declining precipitation and overextraction of water resources.

During the study period from 2014 to 2024, Table 3 reveals variations in the distribution of areas among different drought classes. First, no-drought consistently holds the largest proportion. In 2014, it accounted for 72.90% (3,536.34 km²), which increased to 74.48% (3,612.98 km²) in 2016 and 75.22% (3,648.95 km²) in 2018. However, it slightly decreased to 73.60% (3,570.46 km²) in 2020 before reaching its peak in

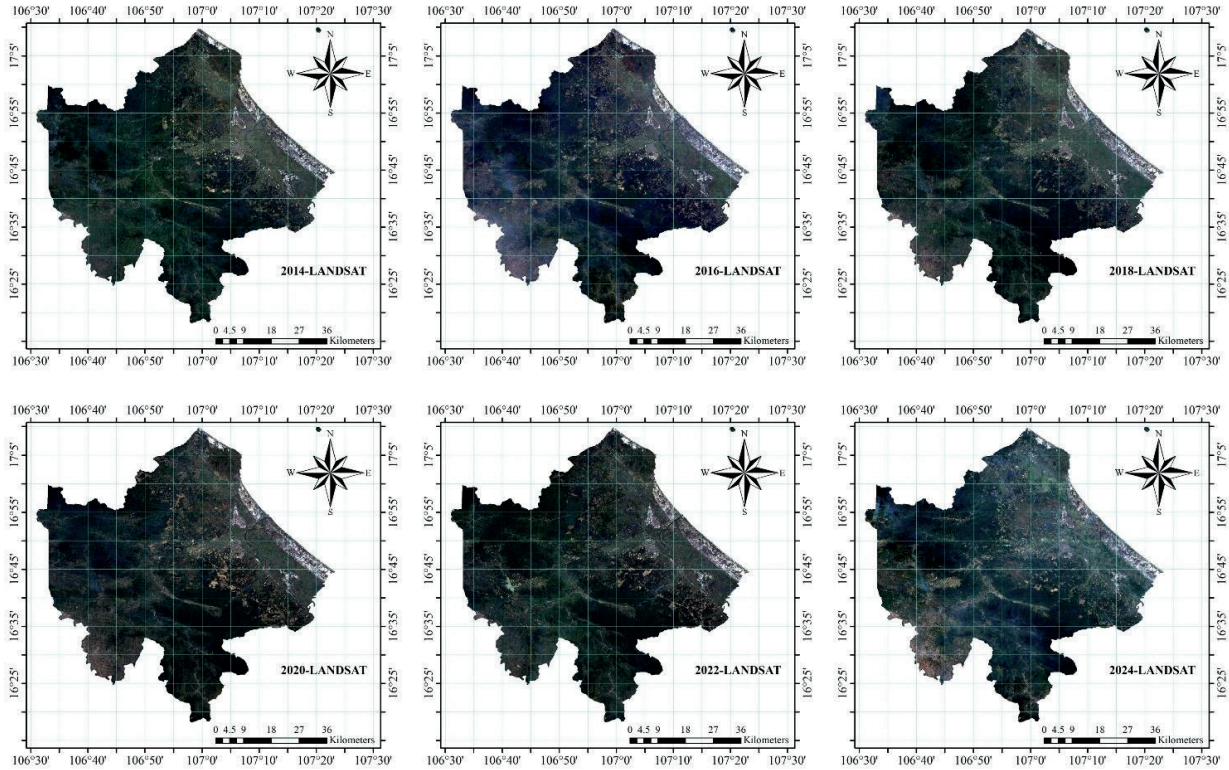

Fig. 3. Landsat data images of Quang Tri province for the period 2014–2024

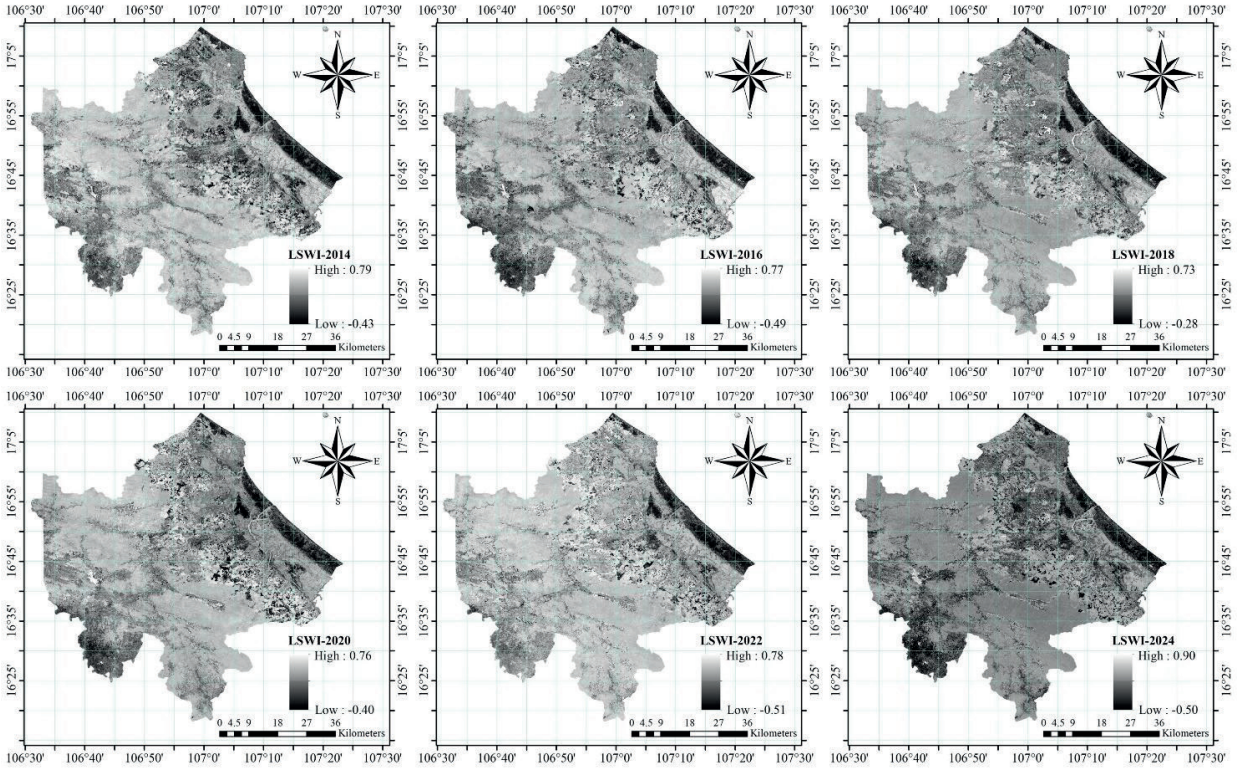

Fig. 4. LSWI maps of Quang Tri province for the period 2014–2024

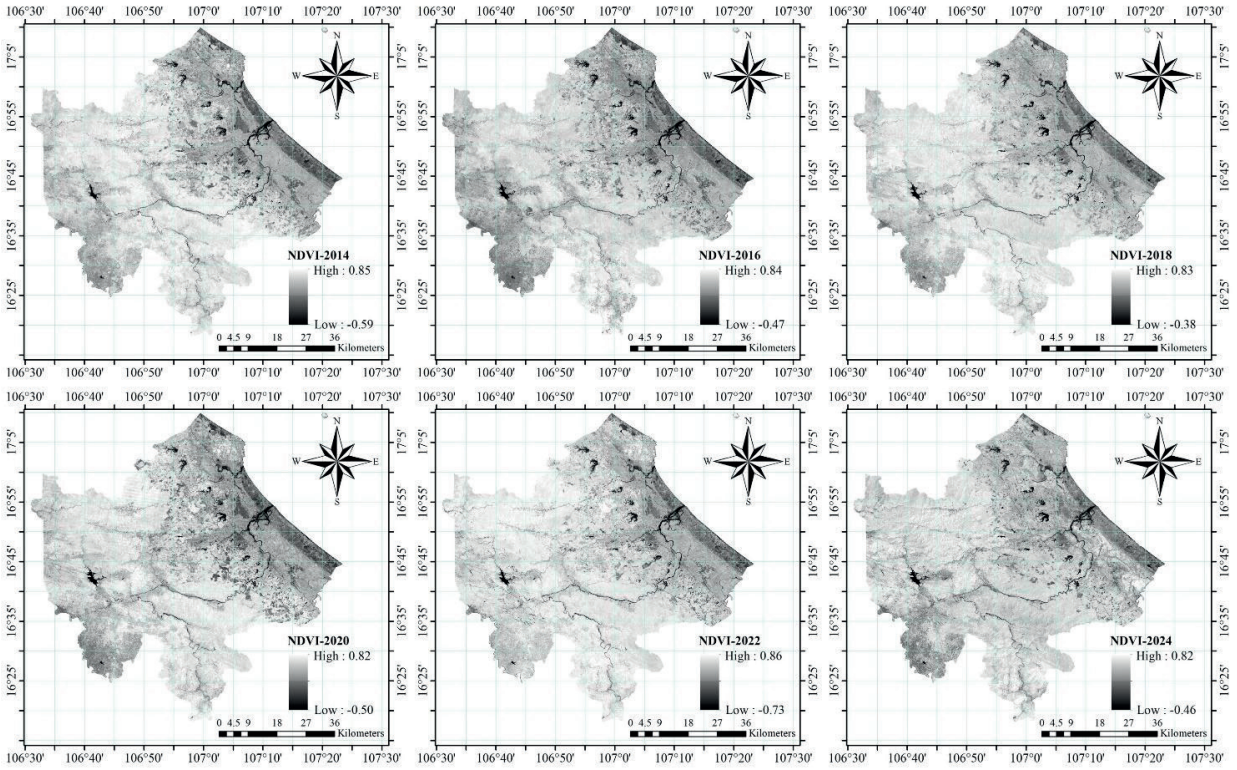

Fig. 5. NDVI maps of Quang Tri province for the period 2014–2024

Citation: Bulletin of Geography. Physical Geography Series 2026, 30, http://doi.org/10.12775/bgeo-2026-0002

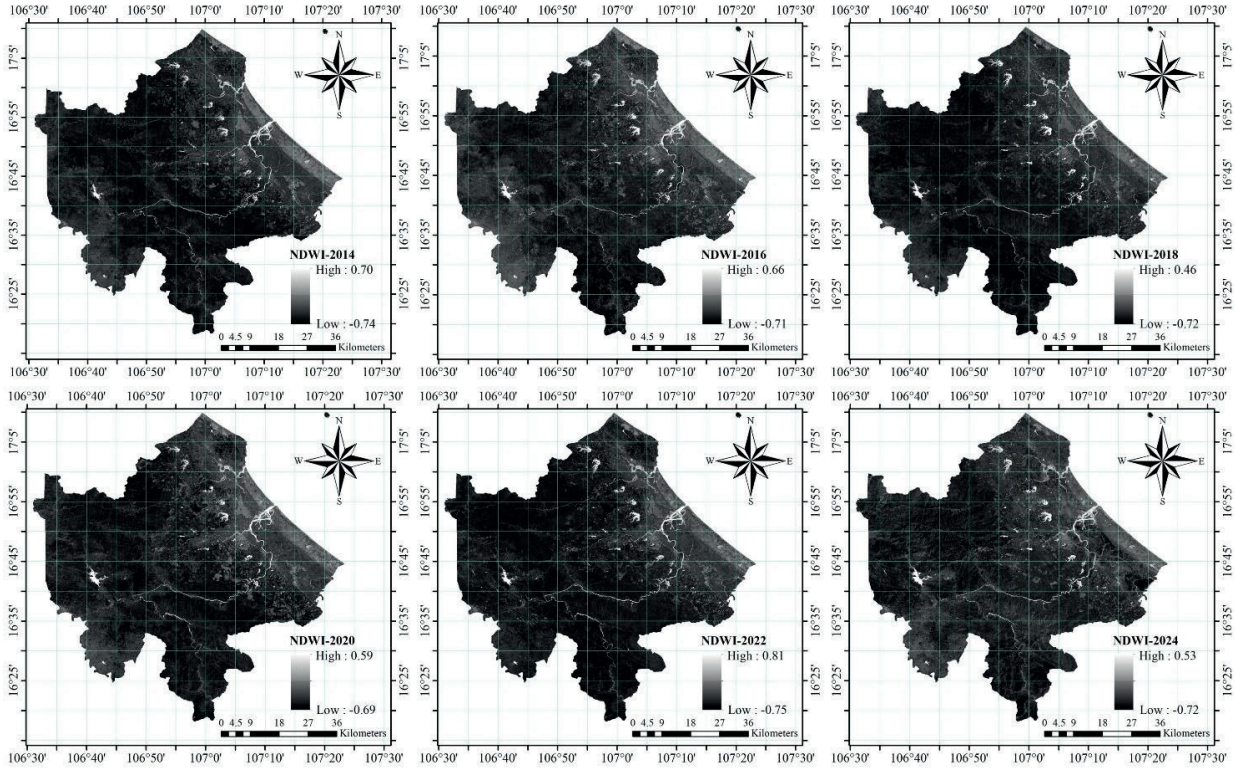

Fig. 6. NDWI maps of Quang Tri province for the period 2014–2024

Table 2. Confusion matrix of the RF model for 2024

	Drought (Prediction)	No Drought (Prediction)
Drought (True)	289	11
No Drought (True)	09	291

2022 at 81.43% (3,950.43 km²). By 2024, this proportion had slightly declined to 74.55% (3,616.61 km²). These fluctuations could be linked to changes in rainfall, temperature and water resource management measures at different times.

Next, mild drought generally decreased from 7.45% (361.58 km²) in 2014 to 4.72% (228.92 km²) in 2024. It fluctuated across the years, with a drop to 4.84% (234.98 km²) in 2016, then a rise to 7.02% (340.39 km²) in 2018. By 2020, it decreased again to 5.51% (267.32 km²) and reached 6.56% (318.34 km²) in 2022 before lowering to 4.72% in 2024. Similarly, moderate drought fluctuated between 4 and 5% in 2014, 2016 and 2018, showing a downward trend to 2.99% (144.89 km²) in 2022 before rising slightly to 4.26% (206.55 km²) in 2024.

Regarding severe drought, although its proportion remains relatively low compared to other classes, noticeable changes were observed. It increased from 2.92% (141.84 km²) in 2014 to 3.27% (158.41 km²) in 2016, then gradually declined to 1.83% (88.91 km²) in 2022, before rising again to 4.47% (217.01 km²) in 2024. Meanwhile, extreme drought fluctuated between 7 and 13% over the study period. In 2014, it accounted for 12.22% (592.57 km²), reaching its highest value in 2020 at 12.99% (630.14 km²). In 2022, extreme drought saw its lowest proportion at 7.18% (348.48 km²) before rising again to 12.00% (581.95 km²) in 2024.

As shown in Table 3, the "No drought" area dominates throughout the study period, peaking at 81.43% in 2022. However, the "Extreme drought" level still maintains a high proportion in several years (12–13%

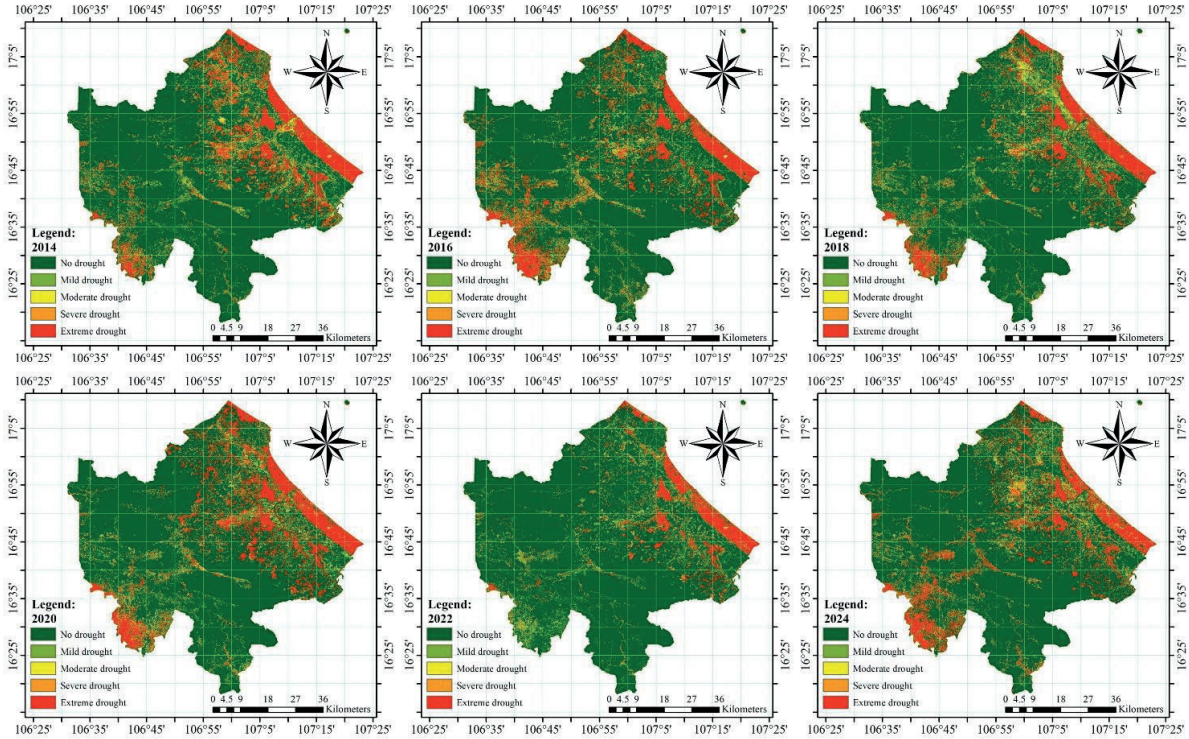

Fig. 7. Drought risk maps of Quang Tri province for the period 2014–2024

in 2014, 2020, and 2024), reflecting that the risk of extreme drought has not been effectively controlled. Other potential factors, such as deforestation or increasing water demand, are discussed as hypotheses and will need to be verified with auxiliary data in future studies.

From these figures, the general trend shows that the area without drought tends to increase significantly in certain years such as 2022. However, the proportion of extreme droughts remains high, indicating that severe drought areas have not been completely mitigated. The results are similar to the annual reports of the province on drought (Quang Tri Province Department of Natural Resources and Environment 2022). These results highlight the importance of water resources management, early-warning systems and sustainable solutions to reduce the damage caused by drought.

Conclusion

This study has classified and analyzed drought severity using multi-temporal remote sensing data, drought indices and machine learning techniques. By integrating Landsat imagery, key drought indices NDVI, NDWI, LSWI and the Random Forest (RF) algorithm on GEE, the research provides a comprehensive

Table 3. Area and percentage of the area of the drought classes during the study period

	No drought		Mild drought		Moderate drought		Severe drought		Extreme drought	
	km²	%	km²	%	km²	%	km²	%	km²	%
2014	3,536.34	72.90	361.58	7.45	218.71	4.51	141.84	2.92	592.57	12.22
2016	3,612.98	74.48	234.98	4.84	223.28	4.60	158.41	3.27	621.40	12.81
2018	3,648.95	75.22	340.39	7.02	212.98	4.39	133.46	2.75	515.27	10.62
2020	3,570.46	73.60	267.32	5.51	218.37	4.50	164.75	3.40	630.14	12.99
2022	3,950.43	81.43	318.34	6.56	144.89	2.99	88.91	1.83	348.48	7.18
2024	3,616.61	74.55	228.92	4.72	206.55	4.26	217.01	4.47	581.95	12.00

drought classification framework for Quang Tri Province over the ten-year period 2014–2024. The results highlighted significant spatial and temporal variations in drought severity, with coastal areas undergoing persistent extreme drought, while central regions showing increasing drought expansion over time. In contrast, western and southern areas remained relatively stable due to better vegetation cover and water availability. The results from this research contributed to a better understanding of drought dynamics and offered valuable guidance for mitigating climate-related risks in vulnerable regions.

Acknowledgment

This work used data from the project: "Application of Google Earth Engine platform and remote sensing data for assessing drought risk in Quang Tri province", code: T25-39. The authors thank the project implementation team and the Hanoi University of Mining and Geology (HUMG) for providing information and data to help the authors complete the research.

Disclosure statement

No potential conflict of interest was reported by the authors.

Author contributions

Study design: TTTT, LHT; data collection: LHT, VPL; statistical analysis: TPTD, VPL; result interpretation: LHT, TPTD; manuscript preparation: LHT, VPL; literature review: TTTT, LHT.

References

AGARWAL V, VISHVENDRA RAJ SINGH BV, MARSH S, QIN Z, SEN A and KULHARI K, 2025, Integrated Remote Sensing for Enhanced Drought Assessment: A Multi-Index Approach in Rajasthan, India. *Earth and Space Science* 12(2): e2024EA003639. DOI: https://doi.org/10.1029/2024EA003639.

AGHAKOUCHAK A, FARAHMAND A, MELTON FS, TEIXEIRA J, ANDERSON MC, WARDLOW BD and HAIN CR, 2015, Remote sensing of drought: Progress, challenges and opportunities. *Reviews of Geophysics* 53(2): 452-480. DOI: https://doi.org/10.1002/2014RG000456.

ALEMU MG and ZIMALE FA, 2025, Integration of remote sensing and machine learning algorithm for agricultural drought early warning over Genale Dawa river basin, Ethiopia. *Environmental Monitoring and Assessment* 197(3): 276. DOI: https://doi.org/10.1007/s10661-025-13059-2.

ALWAN IA and AZIZ NA, 2022, Monitoring of surface ecological change using remote sensing technique over Al-Hawizeh Marsh, Southern Iraq. *Remote Sensing Applications: Society and Environment* 27: 100784. DOI: https://doi.org/10.1016/j.rsase.2022.100784.

BHAGA TD, DUBE T, SHEKEDE MD and SHOKO C, 2023, Investigating the effectiveness of Landsat-8 OLI and Sentinel-2 MSI satellite data in monitoring the effects of drought on surface water resources in the Western Cape Province, South Africa. *Remote Sensing Applications: Society and Environment* 32: 101037. DOI: https://doi.org/10.1016/j.rsase.2023.101037.

BREIMAN L, 2001, Random forests. *Machine Learning* 45(1): 5-32. DOI: https://doi.org/10.1023/A:1010933404324.

CAO R, CHEN Y, CHEN J, ZHU X and SHEN M, 2020, Thick cloud removal in Landsat images based on autoregression of Landsat time-series data. *Remote Sensing of Environment* 249: 112001. DOI: https://doi.org/10.1016/j.rse.2020.112001.

CHANDRASEKAR K, SESHA SAI MVR, ROY PS and DWEVEDI RS, 2010, Land Surface Water Index (LSWI) response to rainfall and NDVI using the MODIS Vegetation Index product. *International Journal of Remote Sensing* 31(15): 3987-4005. DOI: https://doi.org/10.1080/01431160903246736.

COOLEY H, 2006, *Floods and droughts*. Island Press, Washington, DC.

DONG Z, WANG Z, LIU D, SONG K, LI L, JIA M and DING Z, 2014, Mapping wetland areas using

Landsat-derived NDVI and LSWI: A case study of West Songnen plain, Northeast China. *Journal of the Indian Society of Remote Sensing* 42(3): 569-576. DOI: https://doi.org/10.1007/s12524-013-0354-4.

DU TLT, BUI DD, NGUYEN MD and LEE H, 2018, Satellite-based, multi-indices for evaluation of agricultural droughts in a highly dynamic tropical catchment, Central Vietnam. *Water* 10(5): 659. DOI: https://doi.org/10.3390/w10050659.

ELECTRONIC INFORMATION PORTAL OF QUANG TRI PROVINCE, 2025, Geographic location - Natural conditions. Available at: https://www.quangtri.gov.vn/ (Accessed: 15 February 2025).

GAO BC, 1996, NDWI - A normalized difference water index for remote sensing of vegetation liquid water from space. *Remote Sensing of Environment* 58(3): 257–266. DOI: https://doi.org/10.1016/S0034-4257(96)00067-3.

GHOSH S, KUMAR D and KUMARI R, 2022, Cloud-based large-scale data retrieval, mapping, and analysis for land monitoring applications with google earth engine (GEE). *Environmental Challenges* 9: 100605. DOI: https://doi.org/10.1016/j.envc.2022.100605.

GOOGLE EARTH ENGINE (GEE), 2025, Landsat 8 OLI/TIRS. Available at: https://developers.google.com/earth-engine/datasets/catalog/landsat-8 (Accessed: 13 February 2025).

GOOGLE EARTH ENGINE (GEE), 2025, Landsat 9 OLI-2/TIRS-2. Available at: https://developers.google.com/earth-engine/datasets/catalog/landsat-9 (Accessed: 13 February 2025).

GUO Y, LI F, CACCETTA P, DEVEREUX D and BERMAN M, 2016, Cloud filtering for Landsat TM satellite images using multiple temporal mosaicing. *2016 IEEE International Geoscience and Remote Sensing Symposium (IGARSS)*: 7240-7243. DOI: https://doi.org/10.1109/IGARSS.2016.7730867.

GUPTA AK, TYAGI P and SEHGAL VK, 2011, Drought disaster challenges and mitigation in India: strategic appraisal. *Current Science* 100(12): 1795-1806.

IHUOMA SO and MADRAMOOTOO CA, 2019, Sensitivity of spectral vegetation indices for monitoring water stress in tomato plants. *Computers and Electronics in Agriculture* 163: 104860. DOI: https://doi.org/10.1016/j.compag.2019.104860.

KUMAR V, SHARMA KV, PHAM QB, SRIVASTAVA AK, BOGIREDDY C and YADAV SM, 2024, Advancements in drought using remote sensing: assessing progress, overcoming challenges, and exploring future opportunities. *Theoretical and Applied Climatology* 155(6): 4151-4188. DOI: https://doi.org/10.1007/s00704-024-05127-x.

MAYBANK J, BONSAI B, JONES K, LAWFORD R, O'BRIEN EG, RIPLEY EA and WHEATON E, 1995, Drought as a natural disaster. *Atmosphere-Ocean* 33(2): 195-222. DOI: https://doi.org/10.1080/07055900.1995.9649532.

MOHAMMED I, ALWAN I and ZIBOON AR, 2024, Drought in Iraq: remote sensing assessment using LSWI-Index and Landsat imagery. *Engineering and Technology Journal* 42(11): 1475-1485. DOI: https://doi.org/10.30684/etj.2024.147019.

MYNENI RB, HALL FG, SELLERS PJ and MARSHAK AL, 1995, The interpretation of spectral vegetation indexes. *IEEE Transactions on Geoscience and Remote Sensing* 33(2): 481-486. DOI: https://doi.org/10.1109/36.377948.

PHAM MP, NGUYEN KQ, VU GD, NGUYEN TTN, TONG TH, TRINH LH and LE VP, 2022, Drought risk index for agricultural land based on a multi-criteria evaluation. *Modelling Earth Systems and Environment* 8(4): 5535–5546. DOI: https://doi.org/10.1007/s40808-022-01376-9.

QUANG TRI PROVINCE DEPARTMENT OF NATURAL RESOURCES AND ENVIRONMENT, 2022, Biennial climate change report. Available at: https://quangtriclimate.vn/baocaokhihau/baocao21/ (Accessed: 13 March 2025).

SIVAKUMAR MVK, 2005, Impacts of natural disasters in agriculture, rangeland and forestry: an overview. In: Sivakumar MVK, Motha RP, Das HP (eds.) *Natural Disasters and Extreme Events in Agriculture*. Springer, Berlin, Heidelberg: 1-22. DOI: https://doi.org/10.1007/3-540-28307-2_1.

TAMIMINIA H, SALEHI B, MAHDIANPARI M, QUACKENBUSH L, ADELI S and BRISCO B, 2020, Google Earth Engine for geo-big data applications: A meta-analysis and systematic review. *ISPRS Journal of Photogrammetry and Remote Sens-*

ing 164: 152-170. DOI: https://doi.org/10.1016/j.isprsjprs.2020.04.001.

THE NATIONAL AERONAUTICS AND SPACE ADMINISTRATION (NASA), 2025, Landsat Science. Available at: https://landsat.gsfc.nasa.gov/ (Accessed: 13 February 2025).

TRINH LH and VU DT, 2019, Application of remote sensing technique for drought assessment based on normalized difference drought index, a case study of Bac Binh district, Binh Thuan province (Vietnam). *Russian Journal of Earth Sciences* 19(2): ES2003. DOI: https://doi.org/10.2205/2018ES000647.

U.S. GEOLOGICAL SURVEY, 2025, Landsat Products and Data Access. https://www.usgs.gov/landsat-missions (Accessed: 13 February 2025).

VIJAYAKUMAR S, SARAVANAKUMAR R, ARULANANDAM M, RAJENDRAN T and DHANARAJ RK, 2024, Google Earth Engine: empowering developing countries with large-scale geospatial data analysis-a comprehensive review. *Arabian Journal of Geosciences* 17(4): 139. DOI: https://doi.org/10.1007/s12517-024-11948-x.

WEST H, QUINN N and HORSWELL M, 2019, Remote sensing for drought monitoring & impact assessment: Progress, past challenges and future opportunities. *Remote Sensing of Environment* 232: 111291. DOI: https://doi.org/10.1016/j.rse.2019.111291.

WILHITE DA, 2016, Drought as a natural hazard: concepts and definitions. In: Wilhite DA (ed.) *Drought and Water Crises: Integrating Science, Management, and Policy*. CRC Press, Boca Raton.

WILHITE DA, SIVAKUMAR MVK and PULWARTY R, 2014, Managing drought risk in a changing climate: The role of national drought policy. *Weather and Climate Extremes* 3: 4-13. DOI: https://doi.org/10.1016/j.wace.2014.01.002.

XIAO X, MING W, LUO X, YANG L, LI M, YANG P, WANG R, DUAN P, ZHANG C and LI Y, 2024, Leveraging multisource data for accurate agricultural drought monitoring: A hybrid deep learning model. *Agricultural Water Management* 293: 108692. DOI: https://doi.org/10.1016/j.agwat.2024.108692.

YANG L, DRISCOL J, SARIGAI S, WU Q, CHEN H and LIPPITT CD, 2022, Google Earth Engine and Artificial Intelligence (AI): A Comprehensive Review. *Remote Sensing* 14(14): 3253. DOI: https://doi.org/10.3390/rs14143253.

ZHA X, JIA S, HAN Y, ZHU W and LV A, 2025, Enhancing Soil Moisture Prediction in Drought-Prone Agricultural Regions Using Remote Sensing and Machine Learning Approaches. *Remote Sensing* 17(2): 181. DOI: https://doi.org/10.3390/rs17020181.

Received 18 July 2025
Accepted 25 September 2025